Rev. Mexicana Astron. Astrof., 8, 59-62 (1983)

THE OPTICAL EMISSION OF THE SNR 3C400.2

M. Rosado

Instituto de Astronomía
Universidad Nacional Autónoma de México

Received 1983 March 25

RESUMEN

Se obtuvieron fotografías de banda angosta e interferogramas de Fabry-Pérot (FP) de la contrapartida óptica del remanente 3C400.2. Las fotografías en Hα y en [S II] confirman el alto cociente de [S II]/Hα encontrado anteriormente por medio de estudios espectroscópicos. Estas fotografías muestran también un conjunto de filamentos brillantes y angostos colocados en forma de media luna; algunos de estos filamentos están orientados en la dirección radial. La fotografía en [O III] muestra la existencia de un filamento sin contrapartida en Hα. Los datos cinemáticos implican que la distancia a este remanente es de 6.7 ± 0.6 kpc y una velocidad de expansión de 60 ± 10 km s^{-1}. Estos valores implican que el remanente está en su fase radiativa de evolución y que es viejo.

ABSTRACT

Narrow band imagery and Fabry-Pérot interferometry have been performed on the optical counterpart of this remnant. The Hα and [S II] photographs confirm the high [S II]/Hα ratio already found by spectroscopic means in one of the optical filaments. These photographs also show a series of sharp and bright filaments arranged in a crescent-shaped nebulosity; some of these filaments are oriented in the radial direction. The [O III] photograph reveals the existence of a filament without any Hα counterpart. The kinematical data imply a distance of 6.7 ± 0.6 kpc to this remnant and an expansion velocity of 60 ± 10 km s^{-1}. These values imply that the supernova remnant (SNR) is in its radiative phase of evolution and that it has an old age.

Key words: SUPERNOVAE REMNANTS – INTERSTELLAR MEDIUM – FP INTERFEROMETRY

I. INTRODUCTION

The extended radio source 3C400.2 (G53.62 – 2.23) was first suggested to be a SNR by Holden and Caswell (1969) who remarked on its low galactic latitude and its high brightness temperature. Milne (1970) observed its non-thermal nature and obtained a spectral index, $\alpha = -0.6$, for this source. As a consequence, the radio source was identified as a SNR. Its optical counterpart was discovered by van den Bergh, Marscher, and Terzian (1973) who observed faint optical emission consisting of diffuse filaments associated to the radio source. The subsequent spectroscopic work of Sabbadin and D'Odorico (1976) showed that the optical emission was indeed characteristic of SNRs because of its high [S II]/Hα and [N II]/Hα line-ratios.

Since then, several studies have been performed mainly at radio wavelengths (Ilovaisky and Lequeux 1972; Willis 1973; Goss, Siddesh, and Schwarz 1975) and also in the optical region (van den Bergh 1978). These works contributed to a better knowledge of this remnant. At the present time, we know that the radio source is located in a region of high and variable extinction caused by the presence, at the north of the remnant, of the dark nebulae L729, L731 and L737 (Lynds 1962) along the line of sight. These dark nebulae probably absorb most of the northern optical emission. Consequently, the overall structure of this source must be obtained from the radio observations which reveal (Goss *et al.* 1975) an almost spherical shell-type SNR of 35 arcmin of angular diameter. The shell is thought to be thick ($\Delta R/R \sim 0.5$) as Willis (1973) and Goss *et al.* (1975) have deduced, and it has maxima of radio emission at the NE and at the NW sides (the sides closer to the galactic plane); it is possible that this asymmetry could be due to an interaction with the interstellar matter (ISM) and that this interaction governs the present evolution of this remnant. The spectral index of -0.62 ± 0.04 is constant over almost the whole radio source but there is a central depression of the surface brightness that is associated with a steepening of the spectral index.

The optical emission associated to this SNR (van den Bergh *et al.* 1973; van den Bergh 1978) is centered at 1950: $\alpha = 19^h\ 35^m\ 06^s$; $\delta = +\ 17°03'.5$ and appears to consist of rather diffuse filaments, crescent shaped and extending only over 7 arcmin. It is probable that the dark clouds mentioned before, mask the optical emission of the NE and NW radio maxima. Otherwise, the optical filaments correlate quite well with the radio emission; indeed, they are located in a local maximum of radio emission and their curvature corresponds to the shape of the radio source. From the work of Sabbadin and D'Odo-

rico (1976) we know that these filaments are really associated with the SNR because they show the following line ratios: [S II]/Hα ≃ 1.37 ± 0.41 and [N II]/Hα ≃ 1.2 ± 0.36 more characteristic of SNRs. From the sulphur line-ratio the electron density in the shell would be of 316^{+480}_{-220} cm^{-3} if one assumes that the electron temperature of the shock recombination zone is 10^4 °K and if one uses Pradhan (1978) emissivities.

An uncertain parameter of this remnant is its distance and consequently, its linear dimensions. The distance has been estimated by several authors (Milne 1970; Ilovaisky and Lequeux 1972; Willis 1973; Caswell and Lerche 1979) on the basis of their proposed Σ–D relations. These estimates range from 4.3 kpc (Willis 1973) to 6.3 kpc (Caswell and Lerche 1979). Consequently, its linear diameter could range from 39.4 to 48.8 pc. The present work refers to optical observations of these filaments. The potographic imagery performed allows us to have the two-dimensional line-ratios of the optical filaments. The radial velocity field, obtained by means of FP interferometry, gives us information about the kinematical distance to this remnant and the expansion velocity of the filaments.

II. OBSERVATIONS

The observations of the optical filaments associated to this SNR were of two types: narrow band photographic imagery and Fabry-Pérot (FP) interferometry. Both of them were performed at the 2.1 m Cassegrain focus telescope of the Observatorio Astronómico Nacional at San Pedro Mártir, Baja California.

The imagery has been performed by means of a focal reducer (Snyder F/2 objective) coupled with a single stage image tube. Three interference filters have been employed: Hα(λ_0 = 6563 Å, Δλ = 10 Å), [S II] (λ_0 = 6719, Δλ = 16 Å) and [O III] (λ_0 = 5018 Å, Δλ = 9.7 Å). The fiber optics output of the image tube was recorded on 103a-G films. The scale of these photographs is of about 49 arcsec/mm, their angular field of 11 arcmin. Table 1 reports the main characteristics of these photographs. Separate calibrations of the plates were also performed to enable a better analysis of the spatial variation of the line-ratios throughout the optical filaments.

The FP interferometry was performed with the same mounting used for the imagery but with the addition of a FP étalon with a free spectral range of 190 km s^{-1}. The standard exposure times were of about one hour. I obtained three Hα-interferograms which were measured and reduced in the standard way (Courtès 1960). A description of the measurements and reductions can be found in Rosado *et al.* (1982).

III. IMAGERY

Figure 1 (Plate) shows the Hα, [S II] and [O III] emission of this remnant. As we can see from the Hα photographs, the optical emission has two components:

TABLE 1

CHARACTERISTICS OF THE NARROW BAND PHOTOGRAPHS

Plate Number	Filter	Exposure Time (min)
SN 180	[S II]	45
SN 186	Hα	30
SN 190	Hα	30
SN 193	[O III]	35

a diffuse one and a network of sharp filaments oriented not necessarily parallel to the overall curvature; these filaments are bright and quite thin.

The [S II] emission resembles very much the Hα emission in both the diffuse and filamentary components. The Hα and [S II] imagery confirms the spectroscopic work of Sabbadin and D'Odorico (1976) about the high [S II]/Hα line-ratio found in one of the filaments. On the contrary, the [O III] emission is quite different. In fact, the Hα and [S II] filaments do not show any appreciable [O III] emission while, on the other hand, there is at least one filament showing a relatively strong [O III] emission without any Hα counterpart. This filament, 38 arcsec in size is located southwards the Hα and [S II] filaments. Unfortunately, the [S II] photograph does not cover the region where the [O III] filament is located so that one cannot state anything about its [S II] emission. The fact that the [O III] filament does not show any Hα emission excludes photoionization by the nearby star of unknown spectrum HD 105090. A possible explanation to this difference in emissions could be that the [O III] filament were located on a shell of larger diameter than the Hα and [S II] shell; the former defining the true shock front as expected from shock emission. Another interesting possibility could be that the filaments with Hα and [S II] emission have different abundances (and perhaps, different kinematical properties) than the [O III] filaments. This happens in other SNRs such as Cas A (Peimbert and van den Bergh 1971; Chevalier 1978) however, in the present case, the size is considerably larger. Before concluding anything about this abundance effect it seems necessary to know the spectrum of the nearby star, to search by means of [O III] and [S II] imagery, for more of such [O III] filaments and to perform a careful spectroscopic study on both classes of filaments. Further discussion about this must await this observational confirmation.

IV. ANALYSIS OF THE KINEMATICAL RESULTS

The three interferograms obtained cover the whole optical region. Figure 2 (Plate) shows one of them. Unfortunately some of the rings are contaminated by lines of the night-sky near to the Hα line; these are the geoco-

ronal Hα line and the OH lines at λλ6568.6 and 6553.6 Å. Since these lines appear clearly separated from the nebular rings, I could identify and eliminate them. Some of the nebular FP rings show splittings; the splitting pattern is shown in Figure 3 where the center of the radio shell and the center of the crescent-shaped optical nebulosity are also marked. As one can see from this figure, the splittings appear more or less of the same strength. This fact is roughly in agreement with the assumption that the splittings correspond to regions at more or less the same distance from the center of expansion. An inspection of Figure 3 eliminates the possibility that the center of the optical nebulosity were the center of expansion and consequently we can assume that this pattern is consistent with that expected from a shell expanding from the center of the radio source and with its size. The optical nebulosity corresponds only to such regions not absorbed by the northern dark nebulae. On the other hand, the distribution of line splittings is perhaps better explained if the optical filaments were clumps or cloudlets where a shock wave were induced due to the passage of a blast wave (McKee and Cowie 1975). In this case, the line-splitting is a function of the pre-shock density of the cloudlet and consequently, the variations in the strengths of the line-splittings are associated with the variations of the pre-shock density of each particular filament. The fact that there are two different classes of filaments, with different emissions, as discussed before, supports this cloudlet assumption. In both cases, the systemic velocity, V_c, can be obtained from the mean velocities of the splittings. In this way I obtain a systemic velocity of 96 ± 9 km s^{-1} which implies a kinematical distance of 6.7 ± 0.6 kpc which is higher than the distances estimated by simpler $\Sigma - D$ relations (Section I) but which is in fairly good agreement with the distance estimate of Caswell and Lerche (1979), who take into account the exponential decay of the ISM density with the height above or below the galactic plane. In what follows I shall take a kinematical distance of 6 kpc and consequently, a linear radius of 22 pc. On the other hand, the observed splittings correspond to differences in velocities amounting to about 110 km s^{-1}. In order to relate them with an expansion velocity V_{exp}, it is necessary to have some idea about the nature of the filaments. If the filaments are indeed cloudlets affected by the passage of the blast wave, as discussed before, then the line splitting give directly the expansion velocity of the cloudlets. In this case, this velocity amounts to 54 ± 10 km s^{-1}. If instead, the filaments are distributed on the expanding radio shell and we assume in addition, that this is thin and spherical then, the expansion velocity is of about 59 ± 10 km s^{-1}. This value is, within the uncertainties, similar to our first estimate, so that I shall adopt a value of $V_{exp} = 60 \pm 10$ km s^{-1}. This assumption of a spherical shell is supported by the radio maps, however, the radio observations do not seem to justify the additional hypothesis of shell thinness. Indeed, the radio surface brightness is better reproduced with models of volume emissivity of thick shells; however, the Hα photographs show that the filaments are quite narrow and, if they are shells seen edge-on, these must be quite thin. If one identifies the optical filaments with the shock recombination region of the shell, then the assumption of shell thinness is fully justified at optical wavelenths.

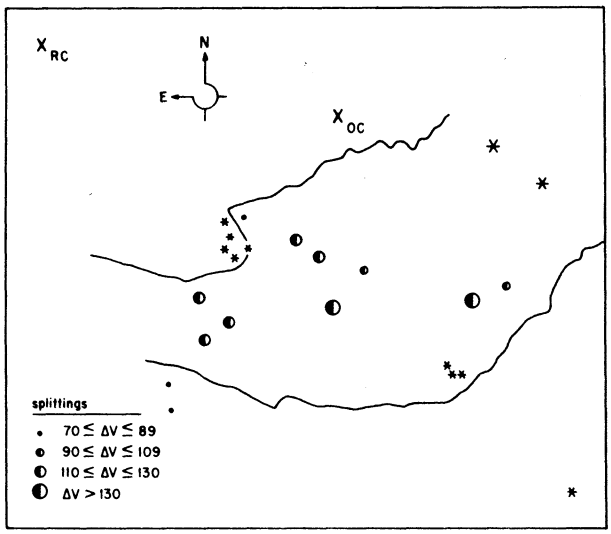

Fig. 3 Splitting pattern of the FP profiles of the optical filaments associated with 3C400.2. The solid lines show the overall crescent-shaped optical nebulosity. OC shows the center of the optical hemisphere while OR shows the center of the radio remnant.

In summary, both the thin shell and the cloudlet assumptions give roughly the same expansion velocity of about 60 km s^{-1} which must be confronted with the spectroscopic data. As I have already discussed in Section I, there are few studies in the optical region. In particular, there is only one work of spectroscopy performed on these optical filaments (Sabbadin and D'Odorico 1976). Since these authors reported only four lines it is not possible to do a reliable shock diagnosis. I have however, compared the observed line-rations with the theoretical models of shock emission of Raymond (1979) and Shull and McKee (1979). From this, one can see that either the models W or X of Raymond (1979) or the models D or E of Shull and McKee (1979) can reproduce the observed values if one takes into account the uncertainties of at least 30% that the observed line-ratios have. This set of models have shock velocities ranging from 81.5 to 100 km s^{-1}; pre-shock densities of 10 cm^{-3}; a wide range of heavy element abundances which could vary from normal (for the models of Shull and McKee 1979) to depleted (for the models of Raymond 1979); and the pre-ionization conditions also vary very much depending on the model.

The expansion velocity derived from the kinematical data is somewhat lower than the values predicted from these theoretical shock models which fit the spectroscopic line ratios. Perhaps this kinematical shock velocity

is only a lower limit, but since we do not have better spectroscopy (and kinematics) I shall adopt this value as representative of the shock velocity, V_s.

The sulphur line-ratio implies an electron density in the filaments of $316 \pm {}^{480}_{220}$ cm^{-3} as discussed in Section I; the large uncertainties in this quantity are due to the fact that the sulphur ratio falls in the low density region ($n_e < 10^3$ cm^{-3}). From this value and from the kinematical expansion velocity one can obtain the pre-shock density, n_0, by assuming that the compressions in the radiative shock are of about $(V_s/C_s)^2$. Taking a sound speed, $C_s = 10$ km s^{-1}, we obtain that $n_0 \simeq 9 \pm {}^{13}_{6}$ cm^{-3}. Another estimate of this quantity can be obtained from the limiting emission measure in the PSS prints in a way discussed by Rosado (1981). Since the filaments are not visible in the PSS, then, the limiting value of n_0, if the emission is due to a shock with a velocity of 60 km s^{-1}, would be $n_0 \lesssim 5$ cm^{-3}. This latter estimate must be, however taken with caution because the filaments could be severely absorbed by dark clouds. From these estimates I shall adopt a value of $n_0 = 4$ cm^{-3}. In summary, the kinematical and spectroscopic data imply the following parameters for the SNR 3C400.2:

$$R_s \simeq 22 \text{ pc}$$
$$V_s \simeq 60 \text{ km s}^{-1}$$
$$n_0 \simeq 4 \text{ cm}^{-3}$$

The parameters, together with the assumption that this remnant is in its radiative phase of evolution (Chevalier 1974) enable us to obtain the initial energy of the SN explosion E_0, of about 1.2×10^{51} ergs, a value which is between the typical values of energies released in SN explosions, and an age of 1.1×10^5 yrs.

V. CONCLUSIONS

1) The narrow-band photographs show that in addition to a diffuse component, there are thin filaments which are associated with the remnant 3C400.2. Some of these are perpendicular to the general curvature of the nebulosity (say, they are radial).

2) These photographs also show that the Hα and [S II] emission correlate well. The filaments with Hα and [S II] emission show no [O III] counterpart and, on the other hand, there is a filament emitting in [O III] that does not show any appreciable Hα emission. This could be interpreted as emission of a spherical shock wave or as an abundance effect as discussed before.

3) The kinematical data imply both, a kinematical distance of 6.7 ± 0.6 kpc and an expansion velocity of 60 ± 10 km s^{-1}.

4) The distance derived is in agreement, within the uncertainties, with the distances obtained from the Σ–D relations when the effect of height above or below the galactic plane is taken into account.

5) The derived expansion velocity which one identifies with the shock velocity, is somewhat lower than that predicted by fitting the scarce spectroscopic data to shock models.

6) These parameters imply that this remnant is in its radiative stage of evolution, that it is rather old and that the initial energy of the SN explosion is of the same order of magnitude than those found for other SNRs.

It would be desirable to pursue studies of this remnant in the optical region by both spectroscopic and interferometric techniques. It would be interesting to compare these results with the X-ray observations of this SNR.

The author is greatly indebted to the Marseille Observatory (France) where the reductions were performed, and to E. Themsel for typing the manuscript.

REFERENCES

Caswell, J.L. and Lerche, I. 1979, *M.N.R.A.S.*, **187**, 201.
Chevalier, R.A. 1974 *Ap. J.*, **188**, 501.
Chevalier, R.A. 1978, *Ap. J.*, **219**, 931.
Courtès, G. 1960, *Ann. d Ap.*, **28**, 683.
Goss, W.M., Siddesh, S.G. and Schwarz, U.J. 1975, *Astr. and Ap.*, **43**, 459.
Holden, D.J., and Caswell, J.L. 1969, *M.N.R.A.S.*, **143**, 407.
Ilovaisky, S.A. and Lequeux, J. 1972, *Astr. and Ap.*, **18**, 169.
Lynds, B.J. 1962, *Ap. J. Suppl.*, 7, 1.
McKee, C.F. and Cowie, L.L. 1975, *Ap. J.*, **195**, 715.
Milne, D.K. 1970, *Australian J. Phys. (Astrophys. Suppl.)*, **23**, 425.
Peimbert, M. and van den Bergh, S. 1971, *Ap. J.*, **167**, 223.
Pradhan, A. K. 1978, *M.N.R.A.S.*, **193**, 89p.
Raymond, J.C. 1979, *Ap. J. Suppl.*, **39**, 1.
Rosado, M. 1981, *Ap. J.*, **250**, 222.
Rosado, M., Georgelin, Y.M., Georgelin, Y.P., Laval, A., and Monnet, G. 1982, *Astr. and Ap.*, **115**, 61.
Sabbadin, F. and D'Odorico, S. 1976, *Astr. and Ap.*, **49**, 119.
Shull, J.M. and McKee, C.F. 1979, *Ap. J.*, **227**, 131.
van den Bergh, S., Marscher, A.P., and Terzian, Y. 1973, *Ap. J. Suppl.*, **26**, 19.
van den Bergh, S. 1978, *Ap. J.*, **220**, 171.
Willis, A.G. 1973, *Astr. and Ap.*, **26**, 237.

Margarita Rosado: Instituto de Astronomía, UNAM, Apartado Postal 70-264, 04510 México, D. F. México.

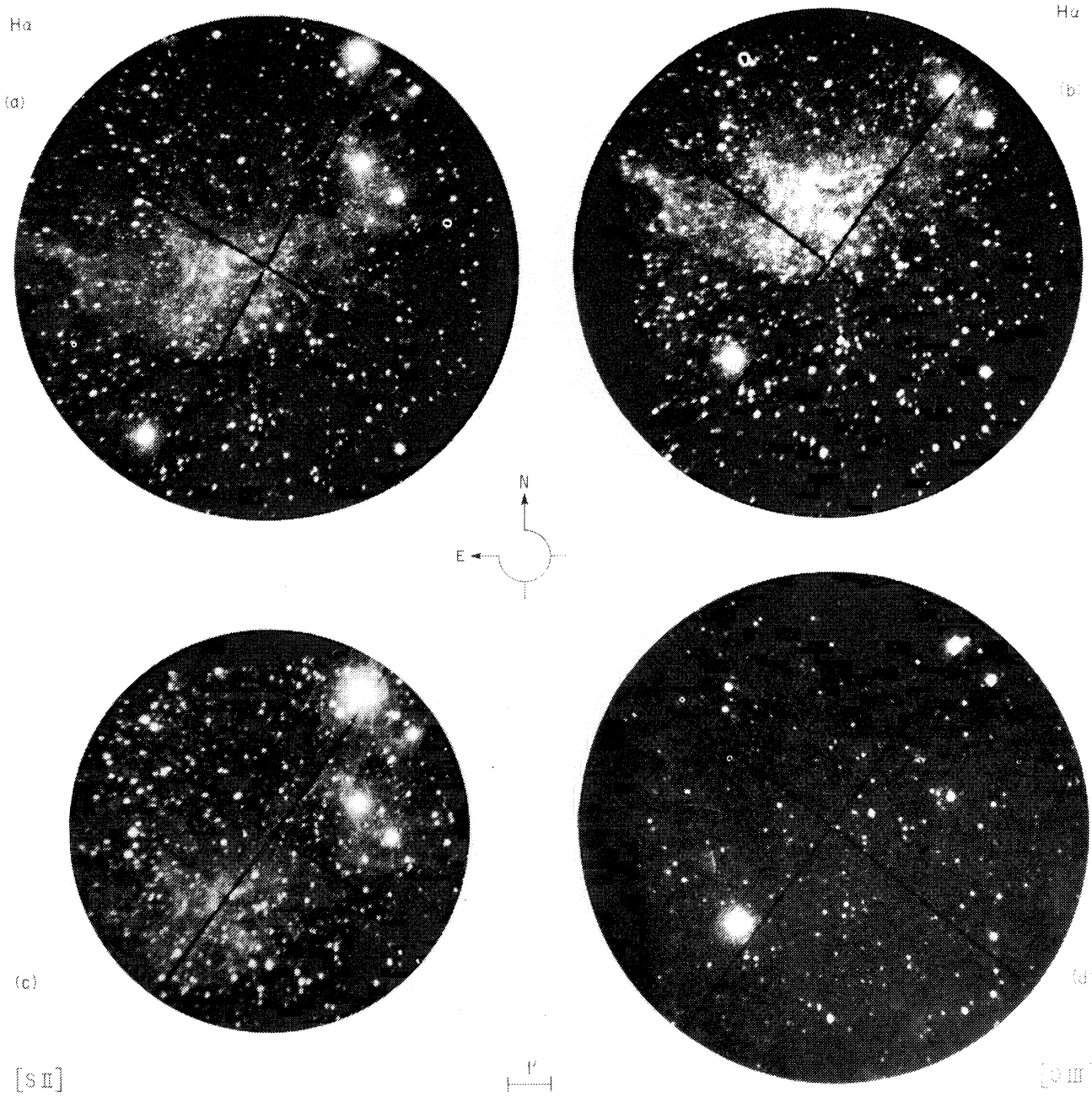

Fig. 1. Narrow-band interference filter photographs of the optical filaments associated with the SNR 3C400.2. a) Hα, b) Hα, c) [S II] (λ6717A), d) [O III] (λ5007 A).

M. ROSADO (See page 59)

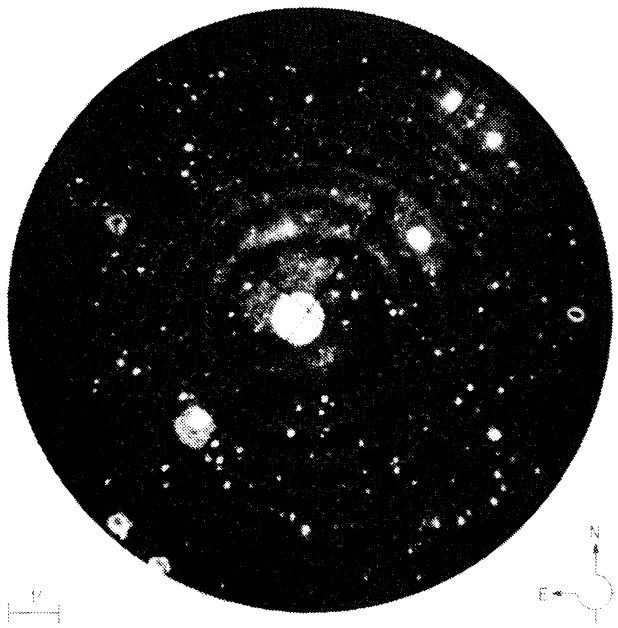

Fig. 2. FP-interferogram, in the light of Hα, of the optical filaments associated with 3C400.2.